Roles of Individual Enzyme−Substrate Interactions by α-1,3-Galactosyltransferase in Catalysis and Specificity[†,‡]

Yingnan Zhang,[⊥] G. Jawahar Swaminathan,[§,$] Ashlesha Deshpande,[§] Ester Boix,[§,#] Ramanathan Natesh,[§] Zhihong Xie,[⊥] K. Ravi Acharya,[§] and Keith Brew*[,⊥]

Department of Biomedical Sciences, Florida Atlantic University, Boca Raton, Florida 33341, USA, and Department of Biology and Biochemistry, University of Bath, Claverton Down, Bath BA2 7AY, UK

Received August 11, 2003; Revised Manuscript Received September 19, 2003

ABSTRACT: The retaining glycosyltransferase, α-1,3-galactosyltransferase (α3GT), is mutationally inactivated in humans, leading to the presence of circulating antibodies against its product, the α-Gal epitope. α3GT catalyzes galactose transfer from UDP-Gal to *β*-linked galactosides, such as lactose, and in the absence of an acceptor substrate, to water at a lower rate. We have used site-directed mutagenesis to investigate the roles in catalysis and specificity of residues in α3GT that form H-bonds as well as other interactions with substrates. Mutation of the conserved Glu^{317} to Gln weakens lactose binding and reduces the k_{cat} for galactosyltransfer to lactose and water by 2400 and 120, respectively. The structure is not perturbed by this substitution, but the orientation of the bound lactose molecule is changed. The magnitude of these changes does not support a previous proposal that Glu^{317} is the catalytic nucleophile in a double displacement mechanism and suggests it acts in acceptor substrate binding and in stabilizing a cationic transition state for cleavage of the bond between UDP and C1 of the galactose. Cleavage of this bond also linked to a conformational change in the C-terminal region of α3GT that is coupled with UDP binding. Mutagenesis indicates that His^{280}, which is projected to interact with the 2-OH of the galactose moiety of UDP-Gal, is a key residue in the stringent donor substrate specificity through its role in stabilizing the bound UDP-Gal in a suitable conformation for catalysis. Mutation of Gln^{247}, which forms multiple interactions with acceptor substrates, to Glu reduces the catalytic rate of galactose transfer to lactose but not to water. This mutation is predicted to perturb the orientation or environment of the bound acceptor substrate. The results highlight the importance of H-bonds between enzyme and substrates in this glycosyltransferase, in arranging substrates in appropriate conformations and orientation for efficient catalysis. These factors are manifested in increases in catalytic rate rather than substrate affinity.

The oligosaccharides of eukaryotic glycoconjugates mediate cellular and molecular interactions, and influence the structures and physical properties of macromolecules (*1, 2*); they also modulate immune responses and have roles in the susceptibility and resistance to pathogens (*3*−*5*). The structures of glycoconjugates produced by a cell are determined by the cellular complement of glycosyltransferases (GTs), enzymes that catalyze that transfer of a monosaccharide from an activated form (often a UDP derivative) into a specific linkage with an acceptor substrate. Families of homologous GTs have been identified with similarities in sequence and/or three-dimensional structure as well as shared sequence motifs (*6*−*9*). Members of such families can differ in donor and acceptor substrate specificity but catalyze the formation of similar linkages between monosaccharides. GTs are of fundamental importance in the field of glycobiology, yet there is limited knowledge of their structures and mechanisms of action.

Two major subgroups of GTs are "retaining" enzymes that catalyze a reaction in which the anomeric configuration of the monosaccharide in the donor substrate (α in UDP-sugars) is retained in the product and "inverting" GTs that reverse the anomeric configuration. These subgroups are expected to differ mechanistically since inverting enzymes can utilize a single displacement mechanism whereas the expected mechanism for a retaining enzyme is two consecutive inverting steps in which the sugar of the donor substrate is initially transferred to a nucleophile and then to the acceptor (*7*). UDP-galactose *β* galactosyl α1,3-galactosyltransferase (α3GT,[1] EC 2.4.1.151) is a retaining trans Golgi-located GT that catalyzes the synthesis of α1,3-galactosyl *β*-OR struc-

[†] This work was supported by Grant GM58773 to K.B. from NIH (USA) and Wellcome Trust (UK) Project Grant 059603 to K.R.A.

[‡] The atomic coordinates for α3GT in complex with *N*-acetyllactosamine and two UDP molecules and the Glu^{317}Gln mutant lactose complex (codes 1O7Q and 1O7O, respectively) have been deposited in the RCSB Protein Data Bank.

* To whom correspondence should be addressed. Phone (561) 297−0407. Fax: (561) 297−2519. E-mail: kbrew@fau.edu.

[⊥] Florida Atlantic University.

[§] University of Bath.

[$] Present address: European Bioinformatics Institute, Wellcome Trust Genome Campus, Hinxton, Cambridge CB10 1SD, U.K.

[#] Present address: Department de Bioquímica i Biologia Molecular, Facultat de Ciències, Universitat Autònoma de Barcelona, 08193 Bellaterra, Spain.

[1] Abbreviations: α3GT, *β*-galactosyl α-1,3-galactosyltransferase; GT, glycosyltransferase; rmsd, root-mean-square deviation; ITC, isothermal titration calorimetry; LacNAc, *N*-acetyl lactosamine; Lac, lactose; Gal, galactose; Glc, glucose.

10.1021/bi035430r CCC: $25.00
Published on Web 10/29/2003

tures in glycoconjugates. This enzyme and its products are found in many mammals, including most primates and New World monkeys but not Old World primates, a group that includes humans (*5*). In these species, the gene encodes an inactive enzyme containing a frameshift mutation (*10*). The absence of active α3GT is thought to be advantageous because it allows the production of natural antibodies (1−3% of circulating IgG) to the product of its action, the α-Gal epitope, which provides an immunologic barrier to infection by certain pathogenic micoorganisms (*11*) and enveloped viruses derived from mammalian hosts that have active α3GT (*4*). The presence of anti-α-Gal antibodies is also a barrier to xenotransplantation of organs (*12*) and with the shortage of human organs for transplantation, genetic manipulation of the α3GT gene (*13*, *14*) and the development of inhibitors of the enzyme are complementary approaches for preventing the rejection of xenotransplanted organs. α3GT is a model for a family of homologous retaining galactosyl- and *N*-acetylgalactosaminyl-transferases that form α-1,3 linkages to *β*-galactosyl and *β*-*N*-acetylgalactosaminyl residues in glycoconjugates. Currently identified relatives of α3GT are the histo-blood group A and B glycosyltransferases (*15*), Forssman glycolipid (Gb_5) synthase (*16*), and isoglo-boside 3 (iGb_3) synthase (*17*).

Previously, we have reported the structure of the UDP complex of α3GT in monoclinic crystal form (form II) at 1.53 Å resolution (*18*). This is at higher resolution and differs from an earlier structure determined from a tetragonal crystal form (*19*) in having a structurally distinct and more ordered C-terminal region. Subsequently, we determined the form II structures of α3GT complexed with UDP-galactose (UDP-Gal), UDP-glucose (UDP-Glc), as well as with both UDP and the acceptor substrates lactose and *N*-acetyllactosamine (*20*). These complexes all contain the Mn^{2+} cofactor that is required for UDP-Gal binding (*21*). Although the UDP-sugars are cleaved into UDP and monosaccharide in their complexes with the enzyme, both monosaccharides remain bound in a solvent-inaccessible location in the active site. Isothermal titration calorimetry (ITC) measurements indicate that donor and acceptor substrates bind in an obligatory ordered manner to the enzyme (*20*).

Here we have investigated the roles of polar residues in the active site of α3GT that make side chain H-bonding interactions with donor and acceptor substrates: Glu^{317}, which interacts with acceptor substrates (*20*) and has been proposed to have a key role in catalysis (*19*), Gln^{247} which forms multiple H-bonds with acceptor substrates (*20*), and His^{280}, that H-bonds with the galactosyl component of UDP-Gal in a modeled enzyme−substrate complex. His^{280} corresponds to a key determinant of donor substrate specificity in the blood group enzymes (*22*). In the absence of acceptor substrate, α3GT catalyzes the transfer of galactose to solvent (UDP-Gal hydrolysis) at a low rate (*21*) and a similar activity has been observed for other GTs (*22*, *23*). Mutants were characterized with respect to catalytic activity for both transferase and UDP-Gal hydrolase reactions, structure and substrate binding. The results indicate that mutational disruption of H-bonding interactions between the enzyme and the donor substrate, UDP-Gal, perturbs the rates of both galactosyltransferase and UDP-Gal hydrolase reactions; disruption of similar interactions with the acceptor substrate selectively perturbs k_{cat} for the transferase reaction. H-bonds have a highly directional character and contribute to enzyme action through effects on substrate orientation and configuration. The crucial role of Glu^{317} in catalysis appears to encompass the electrostatic stabilization of a cationic transition state for cleavage of the UDP to galactose bond and participation in acceptor substrate binding. Structural and mutational studies also clarify the role of a conformational change affecting the C-terminus of α3GT and the role of a second UDP binding site in the enzyme.

EXPERIMENTAL PROCEDURES

Enzyme Expression, Mutagenesis, and Activity Measurements. The catalytic domain of bovine α3GT (residues 80−368) was expressed in *Escherichia coli* BL21(DE3) and purified as described previously (*21*). Mutants were constructed by the polymerase chain reaction megaprimer method (*24*) with minor modifications (*25*) using pET15b-α3GT as a template (*21*). The sequences of mutants were checked by automated DNA sequencing of the expression vector.

Steady state kinetic studies with wild-type and mutant enzymes were performed using a radiochemical assay as previously described (*21*). For characterizing the transferase activity of most mutants, enzyme activity was measured in the presence of 10 mM $MnCl_2$ at a series of UDP-Gal concentrations (generally 0.1−2.0 mM) and different lactose concentrations and the data were analyzed by fitting to the rate equation for a symmetrical sequential initial velocity pattern:

$$v = \frac{V_m[A][B]}{(K_{ia}K_b + K_a[B] + K_b[A] + [A][B])}$$

where [A] is the concentration of UDP-Gal (the first binding substrate in the ordered sequential mechanism of α3GT) and [B] is the concentration of lactose (*18*, *21*). As discussed in the text, in some cases the concentration of UDP-Gal was varied at a single fixed concentration of lactose (generally 25 mM) and lactose was varied at a single fixed concentration of UDP-Gal, generally 1.0 or 1.2 mM. Analysis of these data by fitting to the standard single-substrate Michaelis−Menten equation provided apparent values for K_m for each substrate and two V_m values. The apparent V_m value, obtained by varying [lactose] at fixed [UDP-Gal] was adjusted by multiplying by $(1 + [\text{UDP-Gal}]/K_a)$, where K_a is the apparent K_m for UDP-Gal to get an improved estimate of the true V_m and k_{cat}. This method was used in characterizing the Gln^{247}-Glu mutant which has a low transferase activity relative to UDP-Gal hydrolase activity, as discussed below. UDP-Gal hydrolase activity was determined at a series of UDP-Gal concentrations (generally 0.1−1.0 mM) in the absence of acceptor. The low k_{cat} for UDP-Gal hydrolysis results in this having a rapid equilibrium mechanism as shown by the close agreement between the K_m values for UDP-Gal for the hydrolase activity and K_{ia} values for the transferase reaction in different mutants (Table 4), both of these parameters corresponding to the dissociation constant (K_d) of the enzyme·UDP-Gal complex.

In standard glycosyltransferase activity measurements, the enzyme concentration was 2−5 μg/mL, but 10−20-fold higher concentrations were used with the less active His^{280}

Table 1: Statistics for Data Collection and Refinement

dataset	native enzyme with *N*-acetyl lactosamine + UDP complex	$Glu^{317}Gln$ mutant−lactose complex
cocrystallization conditions	10 mM UDP	10 mM UDP
soaking conditions	50 mM of LacNAc and 20 mM of UDP for 3 h	100 mM of lactose for 3 weeks
wavelength used for data collection (Å) and Synchrotron station	0.87 (PX 9.6-SRS−UK)	0.87 (PX 9.6-SRS−UK)
resolution range (Å)	40.0−1.3	50.0−1.97
space group	$P2_1$ (2 mol/a.u.)	$P2_1$ (2 mol/a.u.)
cell dimensions (Å)	$a = 45.37$ $b = 94.68$ $c = 95.00$ $\beta = 99.03°$	$a = 45.20$ $b = 94.28$ $c = 94.68$ $\beta = 99.10°$
no. of observations	1,062,198	281,132
no. of unique reflections	184,017	55,393
completeness (%)	94.9 (67.7)[a]	99.4 (98.7)[b]
I/σ (I)	15.9 (4.2)[a]	18.1 (10.8)[b]
R_{symm} (%)[d]	5.7 (17.1%)[a]	5.6 (10.5)[b]
R_{cryst}(%)[e]/R_{free}(%)[f]	10.7/15.4	18.1/20.1
deviations from ideality		
bond lengths (Å)	0.013	0.006
bond angles (deg)	1.5	1.3
no. of protein atoms	4,862 (2 molecules)	4786 (2 molecules)
no. of solvent atoms	952	594
glycerol molecules	5	0
ligand molecules	2 normal UDP; 2 additional UDP, 2 LacNAc molecules (on per monomer)	2 normal UDP; 2 Lac (one per monomer)
B-factor statistics (Å^2)		
Wilson B-factor	11.0	16.1
overall B-factor	13.8	54.9
Protein All atoms	10.6	15.5
Protein Main-chain	8.6	14.3
Protein Side-chain	12.4	16.6
Solvent atoms	28.0	25.7
UDP atoms[g]	5.8 (UDP1) 49.9 (UDP2)	11.4 (UDP1)
ligand atoms[h]	10.7	30.7
Mn^{2+} ion[i]	5.0	12.9
mean anisotropy[j]	0.35	

[a] Outermost shell is 1.35−1.30 Å. [b] Outermost shell is 2.04−1.97Å. [c] $R_{symm} = \Sigma_h\Sigma_i [|I_{(h)} - \langle I_{(h)}\rangle|/\Sigma_h\Sigma_i I_{i(h)}]I_{i(h)}$ is the ith measurement and $\langle I_{(h)}\rangle$ is the weighted mean of all measurements of $I_{(h)}$. [d] $R_{cryst} = \Sigma_h|F_o - F_c||/\Sigma_h F_o$ where F_o and F_c are the observed and calculated structure factor amplitudes of reflection h. [e] R_{free} is equal to R_{cryst} for a randomly selected 5% subset of reflections, not used in refinement. [f] All structures have one UDP molecule (UDP1) [except in native enzyme with *N*-acetyl lactosamine + UDP complex which contains second UDP (UDP2) bound to each monomer]. [g] Two LacNAc/Lac molecules (1/monomer). [h] One Mn^{2+} ion bound per monomer. [i] Mean anisotropy calculated using the program PARVATI (*41*).

Table 2: Interactions in Second UDP Site (H-Bonds) in α3GT-*N*-acetyl Lactosamine + UDP Complex

protein atom	UDP atom	distance (in mol 1, Å)
Lys 306 NZ	O3B	2.81
Wat	O3B	2.82
Asp 197 OD2	O2A	2.95
Arg 194 NH2	O2A	3.01
Wat	O1A	3.03
Lys 306 O	O2*	2.29

Table 3: Roles of Residues Selected for Mutagenesis in α3GT[a]

residue	substrate	E atom	S atom	interaction	comment
Gln^{247}	Lac (Gal)	NE2	O4	H-bond	structure
			O5	H-bond	
		(8)		vdw	
His^{280}	UDP-Gal (Gal)	NE2	O2	H-bond	model
Lys^{306}	UDP(2)	NZ	O3 (PB)	H-bond	structure
		O	O2	H-bond	
Glu^{317}	UDP + Gal	N	O4	H-bond	structure
		(3)		vdw	
	Lac (Gal)	OE1	O4	H-bond	
		(3)		vdw	
Arg^{365}	UDP(−Gal)	NH2	O2 P-α	H-bond	structure
		(3)		vdw	

[a] H is hydrogen bond. vdw is van der Waal contact. E atom- enzyme atom. S atom- substrate atom.

mutants. Hydrolase activities were also determined at 10−20-fold higher concentrations (*21*). Both activities in the $Glu^{317}Gln$ mutant were measured using an enzyme concentration of 460 μg/mL (14 μM) and a 60-min incubation time. The hydrolase activity of the $Arg^{365}Lys$ mutant was assayed at 25 μM enzyme and a 60-min incubation time.

The thermodynamics of binding of inhibitors and substrates to α3GT and the Glu317 mutants were characterized by isothermal titration calorimetry using a VP−ITC microcalorimeter (Microcal Inc.) at 30 °C as described previously (*20*). Enzyme was dialyzed against 20 mM Tris HCl buffer, pH 7.5, containing 0.1 M NaCl and 10% glycerol and ligands were dissolved in the same buffer. For measurements of lactose binding, 2 mM UDP and 2 mM $MnCl_2$ were added to the enzyme solution. Data were analyzed using Origin version 5.0 (Microcal Inc.).

X-ray Crystallography. Preparations of the recombinant catalytic domain of α3GT were stored at −20 °C in 20 mM MES−NaOH buffer (pH 6.0) in 50% glycerol. All monoclinic form II crystals (wild-type and the $Gln^{317}Glu$ mutant) were grown at 16 °C by the vapor diffusion hanging drop method as described previously (*18*) by mixing 2 μL of the protein at 5 mg/mL in 20 mM MES−NaOH buffer, pH 6.0,

Table 4: Kinetic Parameters of Recombinant α1,3-GT and Its Variants for the Galactosyltransferase and Hydrolase Reactions[a]

enzyme	wild-type	$Q^{247}E$	$H^{280}Q$	$E^{317}Q$	$R^{365}K$[e]
		Galactosyltransferase Reaction			
k_{cat} (s^{-1})	6.4 ± 0.7	0.14 ± 0.07[c]	0.77 ± 0.08	$(27 \pm 7) \times 10^{-4}$ [d]	0.17 ± 0.01
K_a (mM)	0.43 ± 0.07	0.66 ± 0.02[b]	1.02 ± 0.22	0.13 ± 0.05[b]	0.72 ± 0.06
K_b (mM)	19.9 ± 3.4	20.2 ± 1.9[c]	33.6 ± 7.6	233 ± 85[d]	23.8 ± 1.9
K_{ia} (mM)	0.14 ± 0.03	0.15 ± 0.01	0.89 ± 0.25	0.16 ± 0.03[f]	0.14 ± 0.03
$k_{cat}/K_{ia}K_b$ ($\times 10^6$ $s^{-1}M^{-2}$)	2.3 ± 0.7	0.046 ± 0.023	0.03 ± 0.02	7.2×10^{-5}	0.05 ± 0.01
		Hydrolase Reaction			
k_{cat} (s^{-1}) $\times 10^3$	16 ± 1	11 ± 0.2	<2[g]	0.13 ± 0.01	1.4 ± 0.0
K_a (mM)	0.10 ± 0.00	0.15 ± 0.01	n.d.[h]	0.16 ± 0.03	0.14 ± 0.02
k_{cat}/K_a ($\times 10^3$ $s^{-1}M^{-1}$)	0.16	0.073	n.d.	0.00069	0.010
k_{cat} transferase/hydrolase	400	12	>385	51	121
catalytic efficiency: transferase/hydrolase	14000	630	n.d.	104	5000

[a] The parameters were determined at 37 °C in the presence of 10 mM $MnCl_2$. For the galactosyltransferase reaction, steady state velocities were fitted to the equation: $v = VAB/(K_{ia}K_b + K_aB + K_bA + AB)$, A and B represent the donor and acceptor substrates, respectively. [b] The values for K_m (apparent) for UDP-Gal (K_a) was determined by varying [UDP-Gal] at a fixed lactose concentration of 25 mM. [c] The apparent k_{cat} and K_m for lactose (K_b) were determined by varying [lactose] at a fixed UDP-Gal concentration of 1.0 mM. The apparent k_{cat} was corrected by $(1 + K_a/[\text{UDP-Gal}])$ as described in Experimental Procedures. The high hydrolase relative to transferase activity in $Q^{247}E$ and $W^{314}Y$ increases the uncertainty in these values. [d] Determined by varying [lactose] at 1.2 mM [UDP-Gal]. [e] Values for the transferase activity of the $R^{365}K$ mutant are from ref *18*. [f] These are K_m values for UDP-Gal hydrolysis (see text for discussion). [g] The hydrolase activity of this mutant was too low for quantitative analysis at attainable protein concentrations and the (apparent) k_{cat} was measured using 1.0 mM UDP-Gal. [h] n.d., not determined.

10% glycerol, containing 10 mM UDP and 0.1 mM $MnCl_2$, with an equal volume of a reservoir solution containing 5% PEG 6000 and 0.1 M Tris-HCl, pH 8.0. Single crystals appeared after 3−4 days. The α3GT−*N*-acetyl lactosamine (LacNAc)−UDP complex was obtained by soaking the native crystals prior to data collection with a 50−100 mM solution of LacNAc and 20 mM UDP (excess of UDP) in the crystallization buffer. Before data collection, all crystals were flash-cooled at 100 K in a cryoprotectant containing 10% PEG 6000, 0.1 M Tris-HCl, pH 8.0, 25% glycerol, and appropriate ligands. High-resolution data sets (space group $P2_1$ with two molecules in the asymmetric unit) for the LacNAc−UDP complex (1.3 Å) and the $Gln^{317}Glu$ mutant in complex with UDP and lactose (at ∼2.0 Å) were collected at the Synchrotron Radiation Source, Daresbury, UK (station PX9.6 using a ADSC detector system). Raw data images were indexed and scaled using the DENZO and SCALEPACK modules of the HKL suite (*26*), see Table 1.

Since the cell dimensions were isomorphous with the previously determined form II α3GT·UDP structure (*18*), PDB entry 1K4V (Table 1), these coordinates were used as a starting model. Crystallographic refinement was performed using the program package CNS (*27*). Several rounds of bulk solvent correction, energy minimization, individual isotropic B-factor refinement, simulated annealing and model building using the 'O' program (*28*) were performed until the R_{free} value could not be improved. Appropriate ligands (UDP, lactose, LacNAc, and Mn^{2+} ion) were incorporated into the model after careful observation of the respective electron density map (Table 2). Water molecules were gradually included into the model at positions corresponding to peaks in the $|F_o|-|F_c|$ electron density map with heights greater than 3σ and at H-bond distance from appropriate atoms.

For the LacNAc−UDP complex structure at 1.3 Å resolution, further refinement was carried out using SHELXL-97 (*29*). First CGLS refinement in SHELXL was carried out restraining all the 1,2 and 1,3 distances with the Engh and Huber (*30*) restraints. Initially all the atomic displacement parameters (ADPs) were kept isotropic. The R_{free} value after isotropic refinement of the ADPs was 0.198 and R_{cryst} could not be refined beyond 0.18. The data-to-parameter ratio enabled us to carry out anisotropic refinement on ADPs, leading to vast improvement in the electron density maps. All the alternate conformations were added after initial anisotropic refinement. New atoms added to the molecule were isotropically refined for at least two cycles before they were refined anisotropically. The multiple conformation site occupation factors were refined constraining their sum to be unity. Occupancy of water molecules was constrained as 1.0 or 0.5 depending on their peak heights in the electron density maps. Bulk solvent was modeled using Babinet's principle, as implemented in the SWAT option in SHELXL program. Geometric restraints were set to default values as specified in the program documentation. The final round of refinement was carried out with the addition of H-atoms at riding positions for protein residues only, excluding alternate conformers. The positions of H-atoms were not refined but instead calculated on established geometric parameters. Finally the last round of refinement was carried out using all data, without calculation of R_{free}. The last recorded R_{free} and R_{cryst} for this structure were 0.154 and 0.107, respectively. Analysis of the Ramachandran ($\varphi-\psi$) plot showed that all residues lie in the allowed regions for all the refined structures. The final refinement statistics are included in Table 1.

Form I tetragonal crystals were also grown at 16 °C by the vapor diffusion hanging drop method by mixing 2 mL of the protein at 5 mg/mL in 20 mM MES−NaOH buffer, pH 6.0, 10% glycerol, containing 10 mM UDP and 0.1 mM $MnCl_2$, with an equal volume of a reservoir solution containing 1.6 M ammonium sulfate and 0.1 M Tris-HCl, pH 8.0. Single crystals appeared after 4−5 days. Before data collection, the crystals were flash-cooled at 100 K in a cryoprotectant containing 1.6 M ammonium sulfate, 0.1 M Tris-HCl, pH 8.0 and 25% glycerol. The crystals diffracted only to 3.1 Å resolution (cell dimensions $a = b = 97.02$, $c = 114.7$ Å, space group $P4_12_12$, one molecule in the asymmetric unit and solvent content 67%). Two full datasets (native and crystals soaked with 20 mM UDP) were collected at the Synchrotron Radiation Source, Daresbury, UK (station PX14.1 using a ADSC detector system). Raw data images were indexed and scaled using the DENZO and SCALEPACK

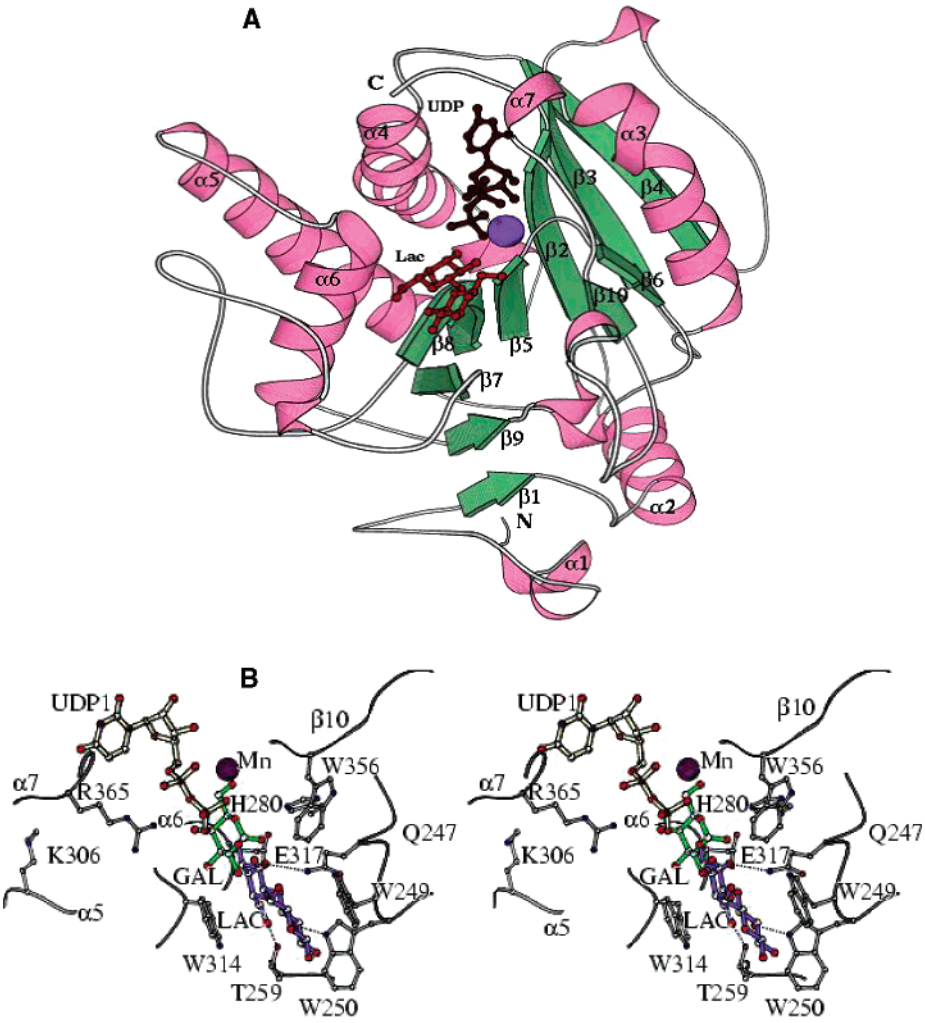

FIGURE 1: Substrate binding sites in α3GT. (A) A ribbon diagram of the overall structure of the complex with Mn^{2+}, UDP, and lactose. (B) A stereo composite representation of bound, cleaved, UDP-galactose and lactose showing the locations of mutation sites discussed in the manuscript. Both figures were generated using MOLSCRIPT (*42*).

modules of the HKL suite (*26*) and the structures were solved using form II α3GT (18, PDB entry 1K4V) as a starting model. Crystallographic refinement was performed using the program package CNS (*27*). Due to limited resolution of the structures, only positional coordinates were refined.

RESULTS

Design and Expression of Mutants. The form II structure of α3GT with the locations of bound UDP, Mn^{2+}, and lactose is shown in Figure 1A. A stereoview of the enzyme active site containing both UDP-Gal and lactose, shown in Figure 1B, shows the enzyme−substrate contacts in greater detail. Gln^{247} is located in the binding site for acceptor substrates and makes two H-bonds with the galactose moiety of lactose and LacNAc. In a modeled complex of α3GT with UDP-Gal, the bound substrate is in a conformation similar to that of UDP-2F-Gal in its complex with the bacterial retaining α-1,4-galactosyltransferase, LgtC, in which the galactose pyranose ring is bent back under the two phosphates and lies nearly parallel to the diphosphate plane (*31*, *20*). An extended conformation of UDP-Gal could not be accommodated in the active site (*20*). In this complex, His^{280}, which does not interact with either substrate in the structures of experimentally determined enzyme.substrate complexes, H-bonds with the galactose 2-OH through NE2 of the imidazole ring H-bonds. This interaction appears to fit with the key role played by the corresponding residue, Met or Leu^{266}, respectively, in the histo-blood group A and B glycosyltransferases in their specificity for UDP−GalNAc and UDP-Gal as donor substrate (*22*). Mutants were constructed with substitutions of Gln, Asn, Thr, Arg, Ala, Gly, Leu, and Pro for His^{280} based on the variability of the residue corresponding to His^{280} in different relatives of α3GT. Glu^{317}, which is conserved in all known relatives of α3GT, is located close to the galactose of the UDP-Gal; its side chain carboxylate forms an H-bond with the 4-OH of the galactosyl moiety of the acceptor. Structurally conservative mutations of Glu^{317} to Gln and Asp were made to try and minimize effects on enzyme structure. The side chain of Gln^{247} H-bonds with O4 and O5 of the galactose component of the acceptor substrate and was conservatively mutated to Glu.

The Gln^{247}Glu, Glu^{317}Asp, and Glu^{317}Gln mutants were all expressed in good yield. Mutants with Leu and Pro substituted for His^{280} expressed in low yield (<1 mg/L of bacterial culture) but others were obtained in yields of 7−12 mg/L. All His^{280} mutants were less soluble than wild-type

Table 5: Thermodynamic Parameters for the Binding of Substrates and UDP to Wild-Type α3GT and Its Variants

ligand titrated	additions	parameter	wild-type	$Q^{247}E$	$E^{317}Q$	$R^{365}K$
UDP (5 mM) + Mn^{2+} (5 mM)	Mn^{2+} (5 mM)	K_d (mM)	0.032 ± 0.001	0.039 ± 0.002	0.12 ± 0.02	0.088 ± 0.004
		Δ*G* (kcal/mol)	−6.23 ± 0.02	−6.06 ± 0.02	−5.44 ± 0.09	−5.62 ± 0.03
		Δ*H* (kcal/mol)	−17.75 ± 0.19	−17.47 ± 0.16	−18.50 ± 0.19	−8.87 ± 0.19
		−*T*Δ*S* (kcal/mol)	11.52 ± 0.19	11.41 ± 0.16	13.06 ± 0.19	3.25 ± 0.19
lactose (100 mM)	Mn^{2+} (2 mM)/UDP (2 mM)	K_d (mM)	2.69 ± 0.06	not detected	not detected	weak binding
		Δ*G* (kcal/mol)	−3.56 ± 0.01	not detected	not detected	weak binding
		Δ*H* (kcal/mol)	−9.29 ± 0.16	not detected	not detected	weak binding
		−*T*Δ*S* (kcal/mol)	5.73 ± 0.16	not detected	not detected	weak binding
UDP-Gal (7.5 mM)	Mn^{2+} (2 mM)	K_d (mM)	0.043 ± 0.001	0.064 ± 0.002	0.31 ± 0.01	not determined
		Δ*G* (kcal/mol)	−6.05 ± 0.01	−5.81 ± 0.01	−4.86 ± 0.02	
		Δ*H* (kcal/mol)	−13.90 ± 0.08	−10.76 ± 0.37	−7.37 ± 0.11	
		−*T*Δ*S* (kcal/mol)	7.85 ± 0.08	4.95 ± 0.37	2.51 ± 0.11	

α3GT and precipitated at concentrations above 1 mg/mL, whereas wild-type enzyme is soluble at concentrations exceeding 5 mg/mL under the same conditions.

Functional Properties of Mutants. (a) $Gln^{247}Glu$. The $Gln^{247}Glu$ mutant shows distinctly different catalytic properties from the wild-type enzyme having greatly reduced galactosyltransferase activity but unchanged hydrolase activity (Table 4). The radiochemical assay measures the combined hydrolase and transferase activities. In calculating the transferase activity, the radioactivity released from UDP-Gal as neutral sugars in the presence of acceptor is corrected using the radioactivity transferred in the absence of acceptor. This correction includes the hydrolase activity, which is reduced in the presence of an acceptor substrate, producing a possible source of error through overcorrection. With the wild-type enzyme, the hydrolase activity is a trivial fraction of the transferase activity and any error is insignificant, but with the $Gln^{247}Glu$ mutant, where the hydrolase activity is about 10% of the combined hydrolase and transferase activities, the potential fractional error in this correction is larger. Consequently, the values determined for the kinetic parameters for transferase activity of this mutant are not entirely satisfactory. However the apparent K_m for UDP-Gal and lactose are similar to those of the wild-type enzyme (Table 5). The K_m and k_{cat} for UDP-Gal hydrolase activity, parameters that can be measured accurately, are essentially unchanged. Therefore, it can be concluded that the effect of this mutation is a 50-fold reduction in k_{cat} for the transferase reaction.

(b) His^{280} Mutants. Under standard assay conditions, His^{280}-Gln has about 10% of the activity of the wild-type enzyme, but the activities of the other mutants were less than 1% of the wild-type enzyme. Their reduced solubility prevented the use of high enzyme concentrations and prolonged incubation times in assays, and detailed kinetic studies were carried out only with the Gln^{280} mutant. The mutation reduces k_{cat} and increases K_{ia} (the K_d for the donor substrate, UDP-Gal). Together, these produce an 80-fold reduction in catalytic efficiency, $k_{cat}/K_{ia}K_b$, (Table 4). The UDP-Gal hydrolase activity of this mutant is less than 1% of the transferase activity, as in wild-type α3GT, and the low activity and solubility did not allow us to determine the K_m and k_{cat} values for UDP-Gal hydrolysis.

Wild-type α3GT has undetectable UDP-GalNAc transferase activity, and all mutants with substitutions for His^{280} were tested for transferase activity with this substrate. Activity was observed in the Ala and Gly mutants which have similar low activities (<1% of wild-type with UDP-Gal) with both UDP-Gal and UDP−GalNAc as donor substrates.

(c) Glu^{317}Mutants. The side chain of Glu^{317} is well positioned to act as the catalytic nucleophile in a double displacement mechanism (*18*−*20*) and electron density adjacent to the carboxyl group in the form I crystallographic structure of a Hg−UDP-Gal complex was initially interpreted as indicating the presence of a covalently bound β-galactosyl group (*19*). However, the structures of α3GT complexes containing both UDP and acceptor substrates indicate that the role of this residue may be complex since it engages in H-bond formation with the 4-OH of the acceptor β-galactosyl group (*20*).

Initial activity assays indicated that mutants with Asp and Gln substituted for Glu^{317} are catalytically inactive. Calorimetric studies showed that the Gln mutant binds UDP similarly to the wild-type enzyme, but the Asp mutant has reduced affinity for UDP and a lower and enthalpy of binding, suggesting that this mutation may affect the structure of the UDP binding site. For this reason, more detailed studies were only performed with the $Glu^{317}Gln$ mutant. Assays using high enzyme concentrations and prolonged incubation times showed that this mutant is active for catalyzing both the transferase and UDP-Gal hydrolase reactions. Transferase activity was characterized by varying [lactose] at a fixed concentration of UDP-Gal (1.2 mM); the effects of varying UDP-Gal concentration on both hydrolase and transferase activities were also measured. Analysis of these data gave the apparent K_m and k_{cat} values shown in Table 4. The value of K_b (lactose K_m) for the galactosyltransferase reaction is tentative because it exceeds the highest concentration of lactose used in the assay. However, the results clearly show that this mutant is deficient in acceptor substrate binding but not in UDP-Gal binding. Its k_{cat} for the transferase reaction is approximately 2400 times lower than that of the wild-type enzyme and the low activity for catalyzing UDP-Gal hydrolysis reflects a 120-fold reduction in k_{cat}, the K_m for UDP-Gal being essentially unchanged.

(d) $Arg^{365}Lys$. This mutant was previously constructed to investigate the role of the flexible C-terminal section of α3GT in its catalytic activity. Its galactosyltransferase activity was previously characterized but not the hydrolase activity. As shown in Table 4, this mutation reduced the k_{cat} for UDP-Gal hydrolysis about 10-fold but has no significant effect on the affinity for UDP-Gal.

Crystallographic Studies. (a) Active Site Conformational Flexibility and Binding Sites in Wild-Type α3GT. Previously, monoclinic and tetragonal crystal forms of bovine α3GT

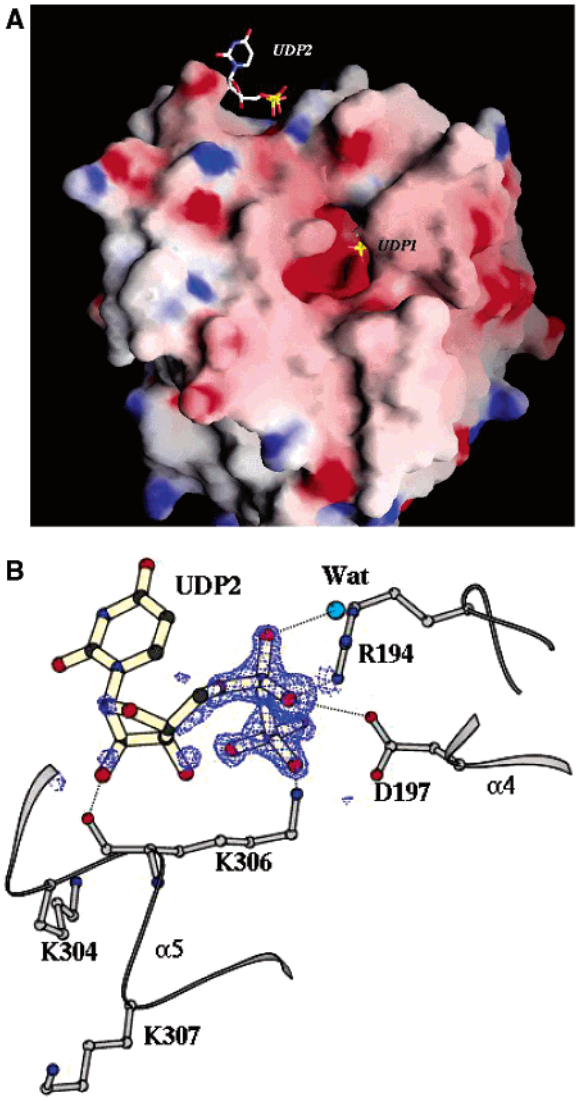

FIGURE 2: The two UDP binding sites of α3GT. (A) Locations of the two UDP binding sites (UDP1 and UDP2) in α3GT. The two UDP molecules are shown as ball-and-stick models and the molecular surface of the protein is colored based on electrostatic charge: red indicates negative charge and blue, positive charge. UDP1 is mostly buried by the C-terminal region of the enzyme. The figure was generated using GRASP (*43*). (B) Details of interactions at the second UDP site (UDP2). The sigma level of the F_o-F_c omit map around the UDP phosphates (blue) is 3.0. This figure was drawn using BOBSCRIPT (*44*).

have been characterized and designated as form I and form II structures, respectively. Form II diffracts at higher resolution (up to 1.3 Å in the present study), is more ordered, and encompasses previously characterized complexes of the enzyme with UDP/Mn^{2+}, UDP-Gal, UDP-Glc, and two acceptor substrates (plus UDP and Mn^{2+}). The form II structure containing UDP/Mn^{2+} has now been refined anisotropically and hence provides better definition of the dynamics of the molecule. This structure reveals the presence of two bound UDP molecules. One (UDP1, Figure 2A) is located at the site previously identified in the enzyme·Mn^{2+}·UDP complex (*18*) through interactions of the uracil with Phe^{134}, Val^{136}, and Tyr^{139} and direct and Mn^{2+}-mediated interactions between the Asp^{225} Val Asp^{227} motif and the ribose and both phosphates. Lys^{359} and Tyr^{361} of the flexible C-terminus interact with the β-phosphate, while Arg^{365} and Tyr^{139} also interact with the α-phosphate. The second UDP (hitherto unidentified UDP2, with partial occupancy, Figure 2) is bound close to Lys^{306} in the vicinity of residues Lys^{304}, Lys^{307}, and Arg^{194}. The density for the ribose ring and the two phosphates are well defined in the electron density map, but the uridine ring appears to be disordered. The oxygen atoms from the phosphates H-bond with neighboring residues, which seems to stabilize the site (Table 2). A LacNAc moiety is also bound as described previously (*20*).

The second UDP site is distant from the Mn^{2+} cofactor that is required for catalysis and from the previously characterized binding site for acceptor substrates (*20*), suggesting that it does not have a direct role in catalysis. This was confirmed by expressing a mutant enzyme in which Lys^{306}, which makes the principal interactions with UDP at the second site, was replaced by Ala. Limited steady-state kinetic studies in which the concentration of donor and acceptor (lactose) substrates were separately varied at a single fixed concentration of the other substrate showed that the apparent K_m values for both substrates and k_{cat} are insignificantly different from the wild-type enzyme (data not shown). It should be noted, however, that this cationic region on the surface of α3GT is conserved in α3GTs from different species, and it is conceivable that it has some role in vivo. Possibilities include lowering the concentration of UDP to reduce enzyme inhibition through formation of dead-end α3GT·UDP·acceptor complexes or retention of UDP in the Golgi lumen for hydrolysis and recycling to the cytosol (*32*).

We have also calculated electron density maps at 3.1 Å resolution for form I crystals of α3GT that were grown in the presence of 10 mM UDP and 0.1 M $MnCl_2$ and subsequently soaked in 20 mM UDP and 20 mM $MnCl_2$. Although these crystals are well ordered, they do not diffract beyond 3.1 Å, even on the Synchrotron source. Analysis of their electron density maps shows a complete absence of density for the polypeptide chain C-terminal to Gln^{357}, indicating that residues Thr^{358} to Val^{368} of the enzyme are disordered. Interestingly, there is no electron density that can be attributed to UDP in the primary binding site, although a small region of density is present that appears to reflect the presence of a bound Mn^{2+} cofactor. These observations provide structural evidence that the conformational change that produces the fixed structure of the C-terminal 11 residues of α3GT present in the form II structure is coupled with UDP binding.

(b) Structure of the $Glu^{317}Gln$ Mutant. The crystallographic structure (form II) of the Gln^{317} mutant in a complex with lactose, Mn^{2+}, and UDP was determined at 1.97 Å (Table 1 and Figure 3). The structure shows that the mutation produces no overall change in structure (root-mean-square deviation of 0.15 Å for the mutant and wild-type structures) and the side chain of residue 317 forms an H-bond with the 4-OH of the β-galactosyl component of the acceptor as in wild-type α3GT. However, when the structures of equivalent complexes of the wild-type enzyme and mutant are superimposed, it can be seen that the mutation perturbs the orientation of the bound lactose (Figure 3). The absence of structural change in the enzyme indicates that the reduction in catalytic activity is a direct result of the change in side chain chemistry in residue 317.

(c) Calorimetric Binding Measurements. The thermodynamics of binding of substrates and the product/inhibitor,

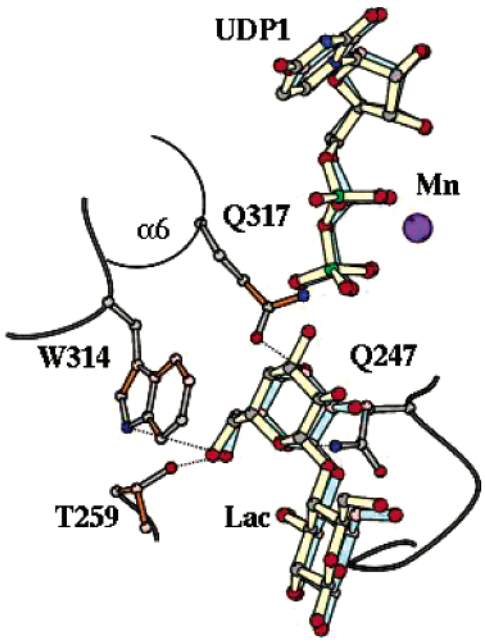

FIGURE 3: Effects of the Glu[317]Gln mutation in α3GT on binding of UDP and lactose. This shows the complex of the Glu[317]Gln mutant with UDP and lactose superimposed with the structure of the corresponding complex of the wild-type enzyme (*20*). The UDP and lactose of the wild-type enzyme are shown in yellow and those from the mutant enzyme in light blue. H-bonds between the mutant enzyme and ligands are shown as dotted lines. The figure was created using MOLSCRIPT (*42*).

UDP, was investigated in the Glu[317]Gln and Gln[247]Glu mutants by ITC for comparison with previously reported data for the wild-type enzyme (*20*) ITC studies with His[280] mutants were unsuccessful because of enzyme precipitation at the concentrations needed for calorimetric measurements. In the Glu[317]Gln mutant, the K_d for UDP is about 4-fold higher than for wild-type α3GT and the binding of UDP-Gal is about 7-fold weaker (Table 5). The affinity of this mutant for UDP-Gal is reduced, reflecting a loss of about 50% of the negative ΔH of binding that is only partially offset by a less negative $T\Delta S$. Lactose binding to the mutant was not detected by ITC, but since the mutant catalyzes galactose transfer to lactose and is found, by X-ray crystallography, to form a complex with lactose and UDP, this appears to reflect a reduced affinity and/or lower ΔH of binding.

ITC studies of the binding of UDP, UDP-Gal, and lactose (in the presence of UDP) to the Gln[247]Glu mutant show that this substitution has a relatively small effect on the affinity for UDP and UDP-Gal. As previously discussed, the stoichiometry of substrate binding cannot be determined under the conditions of these experiments (*20*). However, the similar magnitudes of ΔH of binding for UDP and UDP-Gal for the mutant and wild-type enzymes support the view that this mutant is correctly folded and fully functional for donor substrate binding. However, as with the Glu[317]Gln mutant, lactose binding, in the presence of UDP, was not detected (Table 5) probably because of a low ΔH of binding and/or reduced affinity. This appears to conflict with the unchanged K_m for lactose for this mutant. However, the K_m reflects lactose binding to a catalytically functional enzyme complex containing UDP-Gal, rather than the inhibitory complex with UDP that is used in the ITC experiments.

DISCUSSION

The mechanisms of catalysis and structural basis of catalysis and specificity in glycosyltransferases are not well understood and the mechanisms of retaining glycosyltransferases are particularly controversial (*18*−*22*). The present results provide new information regarding the catalytic mechanism and structure−function relationships in α3GT.

Conformational flexibility appears to be a common feature of glycosyltransferases that is reflected in the structuring of one or more flexible loops on binding the UDP-sugar donor substrate or UDP (*7*, *18*). This has been proposed to help protect the donor substrate from hydrolysis or to facilitate product release, in different enzymes (*7*). The large conformational change in the C-terminal 11 residues of α3GT has been shown to be important for the formation of a binding site for acceptor substrates (*18*, *20*). Here we show that this change, reflected in the structural difference between the form I and form II structures, is closely coupled with the binding of UDP. However, enzyme complexes with UDP and acceptor substrates are dead-end inhibitory complexes that are not directly relevant to the catalytic mechanism. Arg[365], which is conserved in all relatives of α3GT, is important in the transconformation, making interactions with the α-phosphate of the bound UDP, as well as with Tyr[139], Trp[195], and Tyr[361] (*18*). In the Arg[365]Lys mutant, in which the conformational change is expected to be perturbed, the enthalpy of binding for UDP is greatly reduced, in keeping with the role of Arg[365] in UDP binding, while k_{cat} for UDP-Gal hydrolysis and galactosyl transfer to lactose are reduced 12- and 40-fold, respectively (Table 4). These effects imply that the conformational change in the C-terminal region of α3GT has a role in the rate-limiting step for these reactions. The fact that the UDP to sugar bonds are cleaved in the form II complexes of enzyme with UDP-Gal and UDP-Glc suggests that the transconformation is coupled with cleavage of the bond between UDP and C1 of the monosaccharide.

We have also investigated the role of Glu[317] in catalysis by α3GT through the properties of a Glu[317]Gln mutant. This mutation produces a large reduction in catalytic activity but no significant change in active site structure. The K_m for lactose is increased and the ratio of transferase to hydrolase activities reduced, indicating that the effects of the mutation cannot be attributed to the presence of a small proportion of wild-type enzyme, produced by mistranslation, or to partial deamidation of Gln[317]. The large reduction in activity in this mutant indicates that Glu[317] is a key residue in the catalytic activity of α3GT. UDP binding to the enzyme is little affected by the mutation but the enthalpy of binding of UDP-Gal is greatly reduced (Table 5). Therefore, this substitution perturbs the interaction between the enzyme and UDP-Gal, consistent with the effects of the mutation on k_{cat} for galactosyltransferase and UDP-Gal hydrolase activites. The increased K_m for lactose and greater reduction in k_{cat} for the transferase relative to hydrolase activity may be attributable to the change in lactose binding shown in Figure 3 since this alters the location and orientation of the 3-OH group to one that is, presumably, less favorable for deprotonation and galactose transfer.

Because of the location of Glu[317] in the catalytic site and its proposed role in covalent catalysis (*19*), it is important to consider the functional implication of the changes in

enzyme catalytic properties. Previous mutational studies with retaining glycosidases, which catalyze similar reactions to glycosyltransferases, consistently show that substitutions for the catalytic nucleophile (Glu or Asp) reduce k_{cat} for the transferase and hydrolase reactions by 6 orders of magnitude or more. These enzymes include 1,3-1,4-β-glucanase from *Bacillus licheniformis* (*31*), β-glucosidase from *Streptomyces* sp. (*34*), human pancreatic α-amylase (*35*), α-arabinofuranosidase from *Geobacillus stearothermophilus* T-6 (*36*), and β-1,4-glycanase from *Cellulomonas fimi* (*37*), and other enzymes cited in ref *33*. In *Streptomyces* β-glucosidase (*34*) and pancreatic α-amylase (*35*) substituting either Ala or the cognate amide for the wild-type acidic amino acid produces similar effects on activity. The mutation of other key catalytic site dicarboxylic amino acids typically produces much lower reductions in activity. The reductions in activity in the α3GT Gln^{317} mutant therefore strongly suggest that Glu^{317} is not the catalytic nucleophile and, in conjunction with the kinetic properties of α3GT and the structures of α3GT-substrate complexes (*18*, *20*, *21*), support the view that α3GT does not utilize a double displacement mechanism. This also appears to be the case in the bacterial retaining galactosyltransferase, LgtC, which is similar in structure but unrelated in sequence to α3GT (*23*, *31*).

Recently, it was reported that mutation of the residue corresponding to Glu^{317} of α3GT in the homologous blood group glycosyltransferases (Glu^{303}) to Ala reduces the catalytic activity 30 000-fold, but this value appears to be determined under at fixed concentrations of substrates and the detailed functional properties of this mutant were not provided (*22*). On the basis of the increased K_m for acceptor substrate in the Gln^{317} mutant and the inability of the Ala side chain (unlike Gln) to H-bond with the acceptor substrate, it appears that some part of the loss in activity in the blood group transferase mutant results from an increased K_m for acceptor. Glu^{317} is important for catalysis by α3GT, reflected in the 30 000-fold reduction in catalytic efficiency for galactose transfer to lactose (230-fold for transfer to water) in the Gln mutant and is positioned to act in stabilizing a transition state in which the galactose has oxocarbenium ion character in a single displacement S_Ni mechanism (Figure 4 and ref *20*). The micromolar inhibition of α3GT by a 1-*N*-imino derivative of galactose (*38*) is consistent with this although it does not specifically favor a S_Ni mechanism.

α3GT has a more stringent donor substrate specificity than the homologous histo-blood group A and B glycosyltransferases and His^{280} corresponds to a residue that, in these enzymes, has a key role in modulating donor substrate specificity (*22*). Our mutational investigation of the role of this residue in α3GT reveals that, of eight different amino acids substituted at this site, only Gln produces an enzyme with activity greater than 1% of that of the wild-type enzyme. In this mutant, the similar reductions in k_{cat} for the hydrolase and transferase reactions and reduced affinity for UDP-Gal combine to produce an 80-fold loss in catalytic efficiency for each reaction. Therefore, it is reasonable to conclude that this residue facilitates cleavage of the UDP to gal bond. The fact that Gln, like His, at this location can form an H-bond with the 2-OH of the bent conformation of UDP-Gal (Figure 4), provides indirect support for the modeled structure of the α3GT·UDP-Gal complex (*20*). Low levels of GalNAc transferase activity are introduced by substituting amino acids

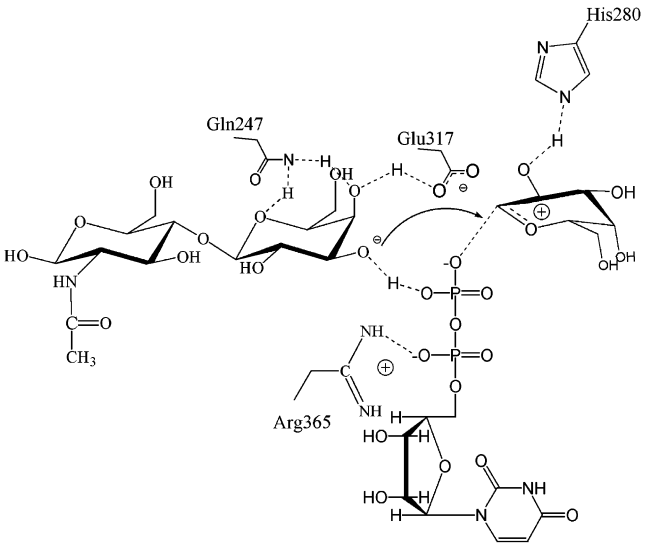

FIGURE 4: Schematic view of transition state in the galactosyltransferase reaction catalyzed by α3GT showing proposed roles of residues mutated in the present study. H-bonds are represented by broken lines.

with small side chains, Ala and Gly, for His^{280}. This suggests that these side chains allow the binding site to accommodate the bulky 2-acetamido group of GalNAc, consistent with the proximity of residue 280 with the 2-position of the monosaccharide ring of the donor substrate. However, the activities of these mutants for both donor substrates are very low, indicating that donor substrate binding is not optimal for efficient catalysis. The effects of substitutions for His^{280} support the idea that an H-bond between the residue at this site and the 2-OH has a key role in donor substrate recognition, in agreement with the finding that the 2-deoxy, 2-F derivative of UDP-Gal, a potent inhibitor of β-1,4-galactosyltransferase, is a relatively poor inhibitor of α3GT (*38*).

A recent report by Lazarus and co-workers (*39*) describes a study in which mutants of porcine α3GT with substitutions of Leu, Ala, Gly, and Arg for His^{271} (corresponding to His^{280} in the bovine enzyme) were expressed in COS and CHOP cells. The cells were probed for cell surface expression of Galα-1,3 Gal structures using a lectin. Their results indicate that the Leu, Ala, and Gly mutants have undetectable activities but they observed lectin binding when the Arg mutant was expressed, although at a reduced level relative to the wild-type enzyme (*39*). This result is puzzling because although we were able to express the His^{280}Arg mutant in high yield, we found it to be devoid of galactosyltransferase activity. The result was checked with independently expressed preparations of enzyme, and the coding sequence in the expression vector was also resequenced. In theory, it is possible that the His^{280}Arg mutation could have different effects in the background of the bovine and porcine α3GTs, but this is extremely unlikely since they are closely similar enzymes with 88% identity in amino acid sequence and His^{280} is a conserved key residue in the active site of α3GTs. Thus, although this previous study describes an interesting alternative approach for screening the effects of mutations on α3GT activity (*39*), the results of our detailed characterization of the purified His^{280}Arg mutant are inconsistent with their findings.

The $Gln^{247}Glu$ mutation in α3GT produces an enzyme with modified acceptor substrate specificity, reflected in a greatly reduced catalytic efficiency for transfer to disaccharide substrates but essentially unchanged catalytic activity for galactose transfer to solvent. Interestingly, the $Glu^{317}Gln$ mutant also perturbs transferase activity much more than hydrolase activity. While Glu^{317}, but not Gln^{247}, is crucial for the hydrolase and transferase activities, both residues H-bond with the galactosyl moiety of the acceptor and, although a structure is not available for the $Gln^{247}Glu$ mutant, it is possible that this mutation perturbs the orientation of the acceptor substrate, as observed for lactose bound to the $Glu^{317}Gln$ mutant (Figure 3).

In α3GT and other glycosyltransferases, the UDP moiety of the donor substrate is a dominant contributor to the energetics of binding. ITC studies give values for the ΔH and ΔG of UDP binding of −17.8 and −6.2 kcal/mol, whereas the corresponding values for UDP-Gal binding are −13.9 and −6.1 kcal/mol, respectively (Table 5). Mutagenesis of His^{280} indicates that donor substrate specificity is determined by the ability of the enzyme to bind only the correct donor substrate in an appropriate conformation for catalysis. This is consistent with the observation that the specificity of the related blood group A and B transferases for UDP−GalNAc and UDP-Gal, respectively, is mediated at the level of catalytic efficiency and not affinity for substrate (*40*). The binding of acceptor in a suitable orientation for galactose transfer is also crucial for the efficiency of the transferase reaction. These aspects of substrate specificity in α3GT are mediated through effects on the stability of the transition state and not Michaelis complexes and are manifested in changes in k_{cat} rather than K_m.

ACKNOWLEDGMENT

We thank the staff at the synchrotron radiation source, Daresbury, UK, for their help with X-ray data collection, Matthew Baker for his contribution to the α3GT project and Shalini Iyer for help during X-ray data collection.

REFERENCES

1. Varki, A. (1993) *Glycobiology 3*, 97−130.
2. Muramatsu, T. (2000) *J. Biochem. 127*, 171−176.
3. Karlsson, K. A. (1995) *Curr. Opin. Struct. Biol. 5*, 622−635.
4. Gagneau, P., and Varki, A. (1999) *Glycobiology 9*, 747−755.
5. Galili, U., Shohet, S. B., Kobrin, E., Stults, C. L., and Macher, B. A. (1988) *J. Biol. Chem. 263*, 17755−17762.
6. Breton, C., Bettler, E., Joziasse, D. H., Geremia, R. A., and Imberty, A. (1998) *J. Biochem. 123*, 1000−1009.
7. Ünligil, U. M., and Rini, J. M. (2000) *Curr. Opin. Struct. Biol. 10*, 510−517.
8. Galili, U., and Swanson, K. (1991) *Proc. Natl. Acad. Sci. U.S.A. 88*, 7401−744.
9. Henrissat, B. (1991) *Biochem. J. 280*, 309−316.
10. Coutinho, P. M., Deleury, E., Davies, G. J., and Henrissat, B. (2003) *J. Mol. Biol. 328*, 307−317.
11. Galili, U. (1989) *Lancet 2*, 358−361.
12. Joziasse, D. H., and Oriol, R. (1999) *Biochim. Biophys. Acta 1455*, 403−418.
13. Morris, P. J. (1999) *Br. Med. Bull. 55*, 446−459.
14. Lai, L., Kolber-Simonds, D., Park, K. W., Cheong, H. T., Greenstein, J. L., Im, G. S., Samuel, M., Bonk, A., Rieke, A., Day, B. N., Murphy, C. N., Carter, D. B., Hawley, R. J., and Prather, R. S. (2002) *Science 295*, 1089−1092.
15. Yamamoto, F., and Hakomori, S. (1990) *J. Biol. Chem. 265*, 19257−19262.
16. Haslam, D. B., and Baenziger, J. U. (1996) *Proc. Natl. Acad. Sci. U.S.A. 93*, 10697−10702.
17. Keusch, J. J., Manzella, S. M., Nyame, K. A., Cummings, R. D., and Baenziger, J. U. (2000) *J. Biol. Chem. 275*, 25308−25314.
18. Boix, E., Swaminathan, G. J., Zhang, Y., Natesh, R., Brew, K., and Acharya, K. R. (2001) *J. Biol. Chem. 276*, 48608−48614.
19. Gastinel, L. N., Bignon, C., Misra, A. K., Hindsgaul, O., Shaper, J. H., and Joziasse, D. H. (2001) *EMBO J. 20*, 638−649.
20. Boix, E., Zhang, Y., Swaminathan, G. J., Brew, K., and Acharya, K. R. (2002) *J. Biol. Chem. 277*, 28310−28318.
21. Zhang, Y., Wang, P. G., and Brew, K. (2001) *J. Biol. Chem. 276*, 11567−11574.
22. Patenaude, S. I., Seto, N. O. L., Borisova, S. N., Szpacenko, A., Marcus, S. L., Palcic, M., and Evans, S. V. (2002) *Nat. Struct. Biol. 9*, 685−690.
23. Ly, H. D., Lougheed, B., Wakarchuk, W. W., and Withers, S. G. (2002) *Biochemistry 41*, 5075−5085.
24. Sarkar, G., and Sommer, S. S. (1990) *Biotechniques 8*, 404−407.
25. Zhang, Y., Malinovskii, V. A., Fiedler, T., and Brew, K. (1999) *Glycobiology 9*, 815−822.
26. Otwinowski, Z., and Minor, W. (1997) *Methods Enzymol. 276*, 307−326.
27. Brünger, A. T., Adams, P. D., Clore, G. M., DeLano, W. L., Gros, P., Grosse-Kunstleve, R. W., Jiang, J. S., Kuszewski, J., Nilges, M., Pannu, N. S., Read, R. J., Rice, L. M., Simonson, T. and Warren, G. L. (1998) *Acta Crystallogr. D54*, 905−921.
28. Jones, T. A., Zou, J. Y., Cowan, S. W., and Kjeldgaard M. (1991). *Acta Crystallogr. A47*, 110−119
29. Shedrick, G. M., and Schneider, T. R. (1997) *Methods Enzymol. 277*, 319−34328.
30. Engh, R. A., and Huber, R. (1991) *Acta Crystallogr. A47*, 392−400.
31. Persson, K., Ly, H. D., Dieckelmann, M., Wakarchuk, W. W., Withers, S. G., and Strynadka, N. C. (2001) *Nat. Struct. Biol. 8*, 166−175.
32. Hirschberg, C. B., and Snider, M. D. (1987) *Annu. Rev. Biochem. 56*, 63−87
33. Viladot, J.-L., Canals, F., Batllori, X., and Planas, A. (2001) *Biochem. J. 355*, 79−86.
34. Vallmitjana, M., Ferrer-Navarro, M., Planell, R., Abel, M., Ausín, C., Querol, E., Planas, A., and Pérez-Pons, J.-A. (2001) *Biochemistry 40*, 5975−5982.
35. Rydberg, E. H., Li, C., Maurus, R., Overall, C. M., Brayer, G. D., and Withers, S. G. (2002) *Biochemistry 41*, 4492−4502.
36. Shallom, D., Belakhov, V., Solomon, D., Shoham, G., Baasov, T., and Shoham, Y. (2002) *J. Biol. Chem. 277*, 43667−43673.
37. MacLeod, A. M., Tull, D., Rupitz, K., Warren, A. J. and Withers, S. G. (1996) *Biochemistry 35*, 13165−13172.
38. Takayama, S., Chung, S. J., Igarashi, Y., Ichikawa, Y., Sepp, A., Lechler, R. I., Wu, J., Hayashi, T., Siuzdak, G., and Wong, C. H. (1999) *Bioorg. Med. Chem. 7*, 401−409.
39. Lazarus, B. D., Milland, J., Ramsland, P. A., Mouhtouris, E., and Sandrin, M. S. (2002) *Glycobiology 12*, 793−802.
40. Palcic, M. M., Seto, N. O. L., and Hindsgaul, O. (2001) *Transfusion Med. 11*, 315−323.
41. Merritt, E. A. (1999) *Acta Crystallogr. D55*, 1109−1117.
42. Kraulis, P. J. (1991) *J. Appl. Crystallogr. 24*, 946−950.
43. Nicholls, A., Sharp, K. A., and Honing, B. (1991) *Proteins Struct. Funct. Genet. 11*, 281−296.
44. Esnouf, R. M. (1997) *J. Mol. Graph. 15*, 132−134.

BI035430R